Self-limiting Nitrogen/Hydrogen Plasma Radical Chemistry in Plasma-Enhanced Atomic Layer Deposition of Cobalt

Ji Liu[a], Hongliang Lu[b], David Wei Zhang[b], and Michael Nolan[a,*]

[a] Tyndall National Institute, University College Cork, Lee Maltings, Dyke Parade, Cork, T12 R5CP, Ireland

[b] State Key Laboratory of ASIC and System, Shanghai Institute of Intelligent Electronics & Systems, School of Microelectronics, Fudan University, Shanghai 200433, China

Corresponding author:

[*]E-mail: Michael.nolan@tyndall.ie. Tel: +353 021 2346983

Graphic abstract

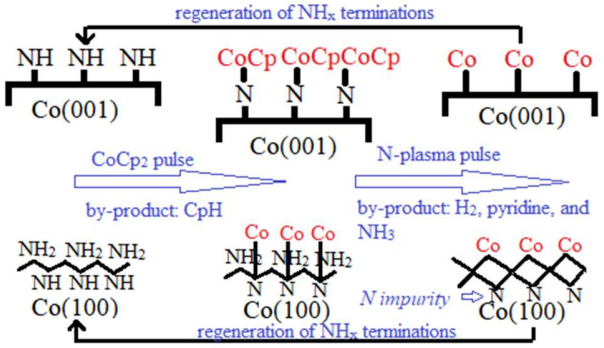

Abstract

Cobalt (Co) is a potential candidate in replacing copper for interconnects and has been applied in the trenches in semiconductor industry over twenty years. A non-oxidizing reactant is required in plasma-enhanced atomic layer deposition (PE-ALD) of thin films of metals to avoid O-contamination. PE-ALD of Co has been demonstrated experimentally with plasma sources of NH_3 or a mixture of N_2 and H_2, but the growth mechanism and key reactions are not clear. In this paper, we have investigated the reactions of plasma generated radicals H, N, NH and NH_2 at metal precursor ($CoCp_2$) terminated Co (001) and (100) surfaces using static DFT calculations at 0 K and molecular dynamics simulations at 600 K. N radicals play an important role in eliminating surface-bound Cp ligand (if any) via pyridine (C_5H_5N) formation and desorption, whereas H radicals have endothermic reactions for eliminating Cp ligand via CpH formation and desorption. The surface NH_x species are eliminated by H radicals via NH_3 formation and desorption. The simulations of these key reactions show that on Co(001) surface, the remaining Cp ligand and surface NH_x species after the metal precursor pulse will be completely removed with N and H radicals, resulting in Co atoms deposited on Co(001) surface at a coverage of 3.03Co/nm^2. Whereas, on Co(100) surface, the surface NH_2 species cannot be completely removed via NH_3

formation and desorption due to overall endothermic reactions. Instead, H radicals react with trench N species, contributed to H transfer at metal precursor pulse, to form NH. These trench N species cannot be eliminated completely on Co(100) surface, which will be the source of N impurities for the deposited Co thin films. At the post-plasma stage, the metal surface will be covered with NH_x-terminations with plasma generated NH radicals, which is then ready for the next deposition cycle. Our results explain why ammonia or H_2/N_2 plasma, which produce NH_x species are required to deposit Co thin films using Co metallocene precursors.

1. Introduction

Copper (Cu) has been used in the semiconductor industry as the interconnect material for over 20 years.[1] However, the continuous deposition of conducting Cu films in the small and complex structures of present and future nanoelectronic device structures is, and will become more difficult. Copper requires a liner or seed layer to promote continuous film deposition. This layer is in addition to the barrier layer, which prevents the diffusion of Cu into the dielectric layer and Si substrates.[2] As device dimensions shrink and more complex structures emerge, the volume available for copper interconnects at the transistor levels becomes correspondingly smaller and must accommodate the barrier, the liner and copper.

From a more general perspective, it is well known that at the nanoscale, Cu will preferentially aggregate into high resistivity 3D island structures.[3-4] One solution to these issues is to replace copper with alternative metals that do not suffer from these issues. In this regard, the early transition metal Cobalt (Co) is of high interest as alternative material for replacing Cu in next

generation interconnects. Co has already been used in the trenches and vias with the downsizing of semiconductor devices.[5-7]

Finding suitable barrier/liner layers and combining these properties into one material is an outstanding challenge because the volume available in trenches and vias exacerbate the issues with copper, so a smaller volume occupied by the barrier and liner layer will help. However, it is clear that copper will ultimately be replaced by another metal.

There is also the question of the deposition of interconnect metals, in particular into high aspect ratio structures in nano-devices, where different surface facets are present and standard physical vapour deposition (PVD) will not give sufficient conformality and uniformity in these structures. Atomic layer deposition (ALD) is widely applied for conformal and uniform deposition offering a high degree of control over deposition at the atomic level, which is required for metal deposition onto high aspect ratio structures.[8-9] Generally, ALD consists of two self-limiting half cycles, where the reactions will stop after all available surface sites are consumed and repeated cycling through the two half reactions allows a fine level of control over the thickness and conformality of the deposited film. In addition to the successful application of ALD in microelectronics and semiconductor industry, it is seeing exciting applications in the areas of catalysis and energy conversion and storage.[6, 10-11]

For the ALD of Co metal, cyclopentadienyl (Cp) based precursors such as the $CoCp_2$ metallocene, $CoCp(CO)_2$ and Co(CpAMD) have been used in thermal and plasma-enhanced ALD.[12-13] For thermal ALD of Co with metal acetamidinates and hydrogen, the required growth temperature can be as high as 350°C, while the growth rate can be as low as 0.12 Å/cycle.[14] With the application of plasma-enhanced ALD (PE-ALD) using NH_3 plasma, the Co PE-ALD process window is between 200°C and 250°C, with a reported growth rate of 0.5 Å/cycle.[15] The reported growth per

cycle with dicobalt octacarbonyl ($Co_2(CO)_8$) and H_2 plasma is increased to 1.2 Å/cycle in the ALD window of 75°C to 110°C.[16] Co metal precursor $CoCp(CO)_2$ has an even larger reported GPC at 1.5 Å/cycle using NH_3 plasma at a higher temperature of 300°C.[17]

The reaction mechanism of film growth with ALD using an oxidizing reactant such as O_3 and H_2O is well-established.[18-21] However, when depositing metals, an O-source will promote oxidation of the metal and therefore cause contamination and severely modify the properties of the metal. To address this issue, non-oxidizing reactants such as NH_3 have been used in PE-ALD of transition metals such as Ta, Ti, Ru and Co.[22-25] For the plasma source, a mixture of N_2 and H_2 is used and the properties of the deposited metal thin film largely depend on the N_2/H_2 gas flow ratio.[23, 26] It has been observed that a H_2 plasma alone or separate N_2 and H_2 plasmas result in high resistivity and low purity Co thin films.[27] Previous studies argue that the presence of NH_x species is needed to deposit low resistivity and high purity Co thin film.[27] These NH_x species are proposed to promote the chemisorption of the metal precursor and the removal of the Cp ligand, analogous to the role of hydroxyl groups in metal oxide ALD[20-21, 28-29]. But they are not incorporated in the film, because the N may desorb in the form of either NH_3 or N_2.

The incorporation of nitrogen into a PE-ALD deposited Co film is temperature-dependent. The formation of CoN_x was reported during the deposition of Co thin films using $CoCp_2$ and NH_3 plasma at temperatures below 300°C[30]. For deposition temperatures above 350°C, decomposition of CoN_x was effectively complete, resulting in pure Co thin films.[30] The detailed mechanism of plasma assisted metal deposition has not yet been established and requires deeper investigations. A plausible proposal is that highly reactive radicals from the hydrogen/nitrogen-plasma source must be present for successful PE-ALD of metals.

A complete PE-ALD process using N-plasma (NH_3 or mixture of N_2 and H_2)[27] can be thought to follow the following process: Firstly, it is vital to note that at the post-plasma stage, the metal surface is actually an NH_x-terminated metal surface, where x = 1 or 2.[31] In the metal half-cycle, the metal precursor $CoCp_2$ reacts with NH_x-terminated metal surface. Cp ligands are eliminated by hydrogen transfer from the surface to form CpH, which desorbs from surface.[32] In the second half-cycle, the plasma generated radicals such as N_xH_y (x = 0, 1; y = 0, 1, 2) will react with the precursor fragments terminated metal surface, eliminating any remaining metal ligands from the surface, and covering the metal surface in some concentration of NH_x groups at the end of second half cycle.

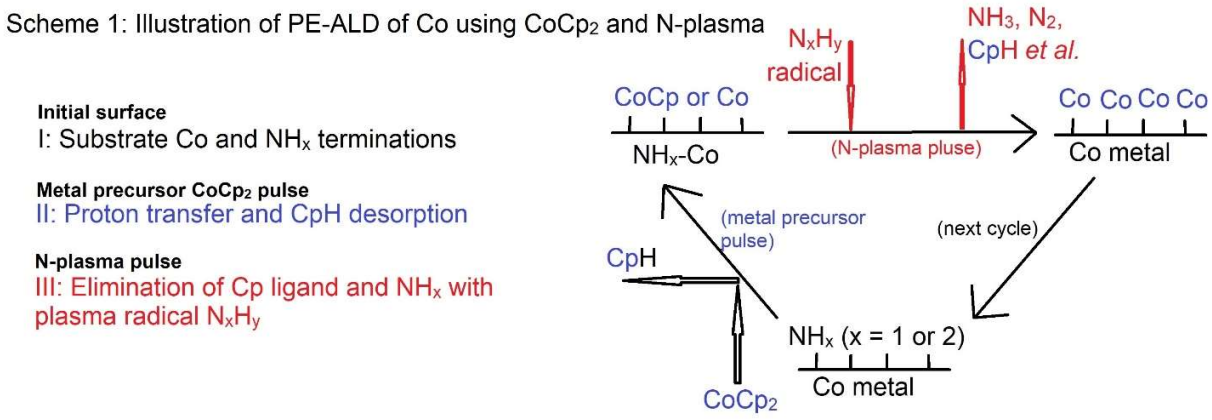

Scheme 1: Illustration of PE-ALD of Co using $CoCp_2$ and NH_3 or N_2/H_2 plasma.

In our recent published work, the nature and stability of NH_x-terminated Co (001) and (100) surfaces and the structures after metal precursor $CoCp_2$ pulse were studied.[31-32] The results show that at typical ALD operating conditions from the literature[5] (temperature range 550K to 650K), the most stable termination of the low energy (001) surface is 0.56ML coverage of NH-termination. On the high energy, zig-zag (100) surface, a mixture of 0.67ML NH and 0.67ML NH_2

is the most stable surface termination. With these NH_x terminations, on the Co(100) surface, the metal precursor can undergo two hydrogen transfer steps and the two Cp ligands are eliminated completely, resulting in Co atom deposition on the surface, whereby Co binds to the N atom. However, on the Co(001) surface, only one Cp ligand is eliminated, resulting in CoCp fragments on the surface after the metal precursor pulse. The computed surface coverage of final terminations after the metal precursor pulse are 3.03 CoCp/nm^2 on NH_x-terminated Co(001) surface and 3.33 Co/nm^2 on NH_x-terminated Co(100) surface.[32]

In the present work, we investigate with density functional theory (DFT) the reactions of plasma generated radicals H, N, NH, and NH_2 with the metal precursor treated Co (001) and (100) surfaces in detail. We use static DFT relaxations at 0 K and *ab* initio MD simulations at 600 K to explore the chemistry of these radicals and how they remove Cp ligands, NH_x species and recover the NH_x terminations needed to promote the metal precursor step.

We find that N radicals play an important role in eliminating surface bound Cp ligands on (001) surface via pyridine formation and desorption and H radicals can promote the elimination of NH_x species on the (001) surface via NH_3 formation and desorption. These reactions are overall exothermic and surface Cp ligand and NH_x species can be removed completely on (001) surface, resulting in deposited Co atoms on (001) surface at a coverage of 3.03 Co/nm^2. Further, plasma generated NH_x species can then cover the (001) surface by reacting with the deposited Co atoms to make new Co-N bonds.

However, on the (100) surface, the surface NH_2 species cannot be fully removed via NH_3 formation and desorption due to an overall endothermic reaction pathway. H radicals contribute to transform bare N species in the (100) trench sites to NH. This current paper shows that these N species are potential sources of N impurities in Co thin film deposition with PE-ALD.

These findings confirm that the plasma radicals play a crucial role in adsorbing metal precursor $CoCp_2$ with the formation of NH_x-terminations on metal surfaces, and the elimination of any remaining Cp ligands that cannot be completely removed during the metal precursor pulse. For Cp-based metal precursors, NH_x species are required to deposit Co thin film with high purity and low resistivity, which explains why NH_3 plasma or a mixture of N_2 and H_2 plasma are the most favourable sources for Co deposition, rather than H_2 plasma or N_2 plasma alone.

2. *Methods and Computational Details*

All the calculations are performed on the basis of periodic spin-polarized density functional theory (DFT) within a plane wave basis set and projector augmented wave (PAW) formalism[33], as implemented in the Vienna *ab initio* simulation package (VASP 5.3) code[34]. The generalized gradient approximation (GGA) with the parameterization of Perdew-Burke-Ernzerhof (PBE) is used for the exchange-correlation functional.[35-36] We use 9 valence electrons for Co, 5 for N, 4 for C, and 1 for H. The plane wave energy cut-off is 400eV. The convergence of energy and forces are set at 1×10^{-4}eV and 0.01eV/Å, respectively. The bulk Co crystal structure is optimized by simultaneously relaxing the ionic positions, cell volume and cell shape at a higher plane wave energy cut-off of 550eV and using a Monkhorst-Pack grid k-point mesh[37] of 12 × 12 × 6. The resulting lattice constants are a = b = 2.49Å, and c = 4.03Å, which are in good agreement with experiment.

The deposited Co films by PE-ALD are polycrystalline and have random surface orientations after low temperature deposition. Based on our previous study[31] on the stability of NH/NH_2 terminations, we have chosen the most stable (001) surface and a less stable but high reactivity

surface, namely (100), to investigate the precursor reaction mechanism. A (4×4) supercell is used to model the (001) surface with a surface lattice of a = b = 9.96Å (surface area = 0.99 nm^2), while a (3×3) supercell, with a surface lattice of a = 7.47Å, b = 12.10Å (surface area = 0.90 nm^2), is used to model the (100) surface. For the Co(001) surface, a five-layer slab is used, with the bottom three layers fixed during the calculation; while for the Co(100) surface, due to its zigzag structure, a four-bilayer (eight-atomic-layer) slab is built with the bottom two bilayers (bottom four layers) fixed during the calculations. From our previous studies, fixing these-layers is sufficient to model these Co surfaces.[31] A k-point mesh[37] of 2 × 2 × 1 is used in (4×4) supercell and for the (3×3) supercell a 3 × 2 × 1 mesh is used. The van der Waals correction was applied with the PBE-D3 method to ensure an accurate description of the dispersion interactions in the computed adsorption energies.[38] Charge transfer is analysed with the Bader charge analysis procedure.[39-40] This was computed from the difference between the Bader charge and the number of valence electrons.

From our previous study, after the metal precursor ($CoCp_2$) pulse, the surface terminations are CoCp fragments on NH_x-terminated Co(001) surface at a coverage of 3.03 CoCp/nm^2 and deposited Co atoms on NH_x-terminated Co(100) surface at a coverage of 3.33 Co/nm^2. These configurations after the metal precursor pulse are shown in Figure 1. On the Co(100) surface, mixed NH_x terminations with NH occupying trench sites and NH_2 occupying surface sites are determined.[31] Trench NH species contribute to eliminate Cp ligands during the metal precursor pulse, resulting in bare N atoms on trench sites (Figure 1(b)).

During the plasma step, the plasma generated radicals H, N, NH, and NH_2 can remove any surface bound Cp ligands and surface NH_x species. At the post-plasma stage, the metal surfaces are supposed to be covered with NH_x-terminations, which is then ready for the next deposition cycle.

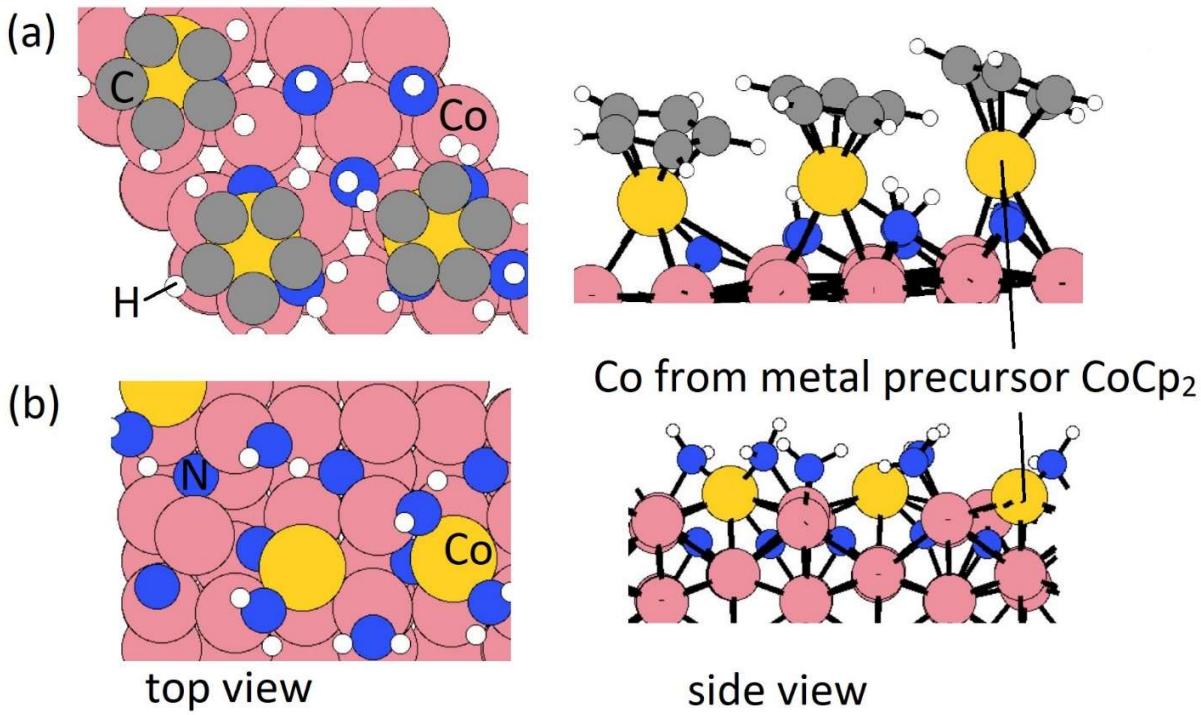

Figure 1. The configurations of final structures on Co (a) (001) and (b) (100) surfaces after metal precursor pulse. Carbon, nitrogen, and hydrogen atoms are presented by grey, blue, and white colour. Substrate Co and Co from $CoCp_2$ are represented by orange and yellow spheres, respectively.

3. *Results and Discussions*

3.1 Reactions of one plasma radical with one CoCp fragment on NH_x-terminated Co(001) surface

As a starting point, to assess the chemistry of the possible radicals from the plasma, we have performed static DFT relaxations of a single plasma radical, that being H, N, NH, or NH_2, which reacts with the Co (001) surface terminated with one CoCp fragment.[32] These results are summarized in Table S1.

The reaction energies are calculated by

$$\Delta E = E_{total} - E_{sub} - E_{plasma} \qquad (1)$$

where E_{total} is the energy of the CoCp-NH_x-terminated Co surface after introducing the plasma radicals. E_{sub} represents the energy of the CoCp-NH_x-terminated Co surface. E_{plasma} is the energy of the plasma generated radicals H, N, NH, and NH_2. In this study, H and N radicals are referenced to half of H_2 and N_2 while NH or NH_2 radicals are referenced to ½(N_2+H_2) or (½N_2 +H_2), respectively, which is consistent with our previous thermodynamic study of NH_x-terminations.[31]

To investigate the formation of CpH from a single bound CoCp on the Co(001) surface, one hydrogen radical is placed near Cp, with an initial C-H distance of 1.90Å. The initial structure and the relaxed stable structure are shown in Figure S1. After relaxing, CpH is formed spontaneously, with a computed positive reaction energy of 1.93eV using equation (1) and C-H bond distance of 1.1Å. The computed energy cost of removing the CpH, resulting one Co atom deposited on the (001) surface, is 2.77eV. After this, the Co-N distance on the surface is 1.73Å, which is slightly shortened compared to surface-terminated CoCp with Co-N distance at 1.74Å. The removal of Cp ligand for one CoCp fragment on Co(001) surface via CpH formation and desorption is overall endothermic with an energy cost of 4.70eV, so this pathway is not a favourable pathway for eliminating Cp ligand at plasma cycle and we therefore do not expect release of CpH during the plasma half reaction.

An alternative chemistry is that N or NH radicals can react with a Cp ligand and insert into a C=C bond to form pyridine (C_5H_4N) or the pyridinium cation (C_5H_5NH). The configurations of relaxed structures after inserting single N or NH radical into a C=C bond of the Cp ligand are shown in Figure S2; the computed reaction energies in these cases are -0.07eV for pyridine and 0.23eV for pyridinium. The computed energy cost of removing pyridine or pyridinium, resulting one Co atom deposited on the surface, are 2.39eV and 2.77eV, respectively. Pyridine has overall less positive

reaction energies and is less endothermic than pyridinium and CpH, so we could expect pyridine as the primary elimination product during the plasma cycle.

Turning now to the surface NH_x species, these can be removed via successive hydrogenation NH ⇒ NH_2 ⇒ NH_3 with H radicals. We consider firstly that the Cp ligand is present throughout the process of elimination of surface NH species on the Co(001) surface terminated with a single CoCp fragment. The reaction energies along the elimination of NH_x species are calculated by

$$\Delta E = E_{total} - E_{sub} - n * E_H + m * E_{NH3} \qquad (2)$$

where E_{total} and E_{sub} are the energies of plasma H radical treated CoCp-NH_x-terminated Co (001) surface and the single CoCp-NH_x-terminated Co (001) surface, respectively. E_H is the energy of plasma generated H radical, which is referenced to half of H_2. E_{NH3} is the energy of NH_3 that desorbs from metal surface.

One H radical is placed near one surface NH species with an initial N-H distance of 1.5Å, where the Cp ligand is present on the surface. The configurations of the initial and relaxed stable structures are shown in Figure S3. The intermediate NH_2 is formed spontaneously, with a positive reaction energy of 1.21eV and N-H bond distance of 1.0Å. We then add an additional H radical near this NH_2 species. After relaxing the structure, NH_3 is formed spontaneously, with an energy gain of -0.51eV and the computed energy cost of the NH_3 desorption is 0.80eV. The removal of first NH species on Co(001) surface with the presence of one CoCp fragment via NH_3 formation and desorption is overall endothermic with an energy cost of 1.50eV.

Figure 2 shows the reaction pathway for elimination of up to 4 NH surface species via NH ⇒ NH_2 ⇒ NH_3 for the case in which the Cp ligand is present throughout. This pathway is overall endothermic. The computed reaction energies for intermediate NH_2 formation, by-product NH_3

formation and desorption are positive in the range of 0.06eV to 1.07eV, except for the 3rd NH_3 formation, which has an exothermic energy at -0.19eV. The configurations of structures along the pathway are shown in Figure S4.

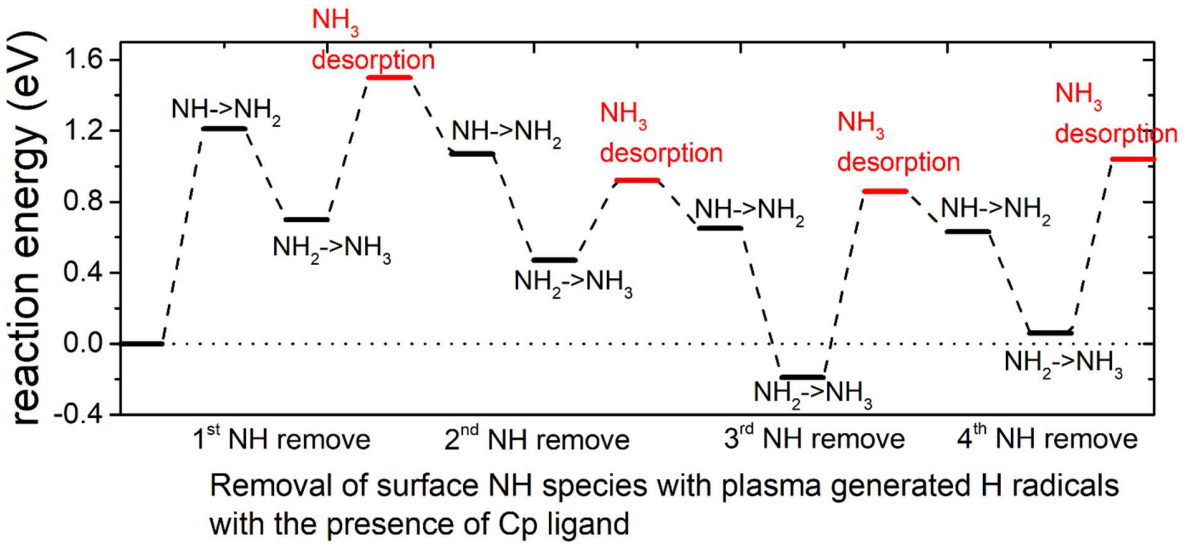

Figure 2. The plotted reaction pathway for removal of surface NH species with plasma generated H radicals with the presence of Cp ring on one CoCp-terminated Co(001) surface. The energy of Co(001) surface with NH_x-termination and one CoCp fragment is set to be the reference energy at 0eV.

The alternative situation is that Cp is first eliminated as pyridine and in Figure 3, we show the reaction pathway for this case. Now the reactions of intermediate NH_2 formation and by-product NH_3 formation and desorption are overall exothermic, except for the initial removal of Cp ligand and NH_3 desorption. The computed energy cost of NH_3 desorption are in the range of -1.41eV to 1.86eV. The positive energy cost is still likely to be overcome by the energy available from plasma-generated excited H radicals at plasma operating condition. The configurations of structures along the pathway are shown in Figure S5.

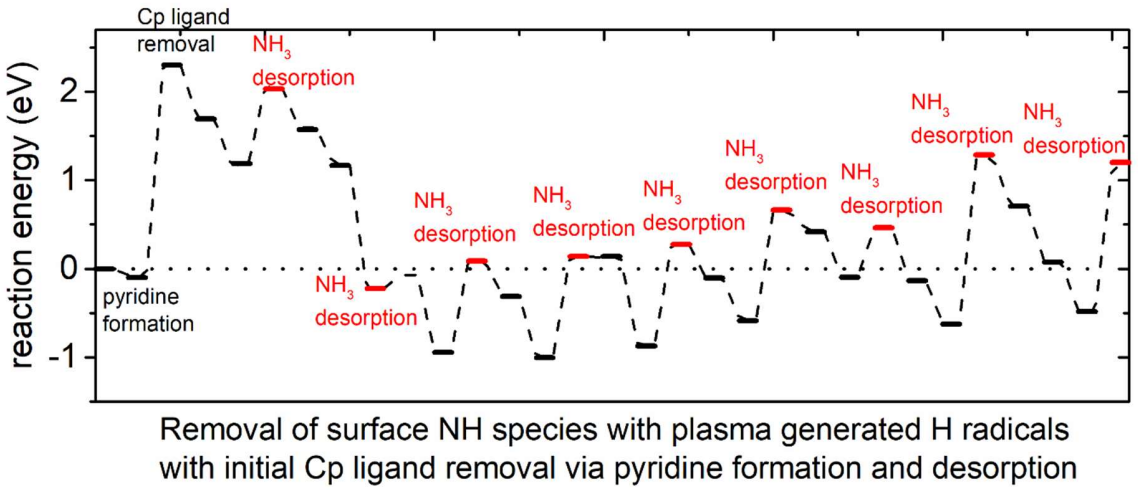

Figure 3. The plotted reaction pathway for removal of surface NH species with plasma generated H radicals with initial Cp ligand removed on one CoCp-terminated Co(001) surface. The energy of Co(001) surface with NH_x-termination and one CoCp fragment is set to be the reference energy at 0eV. The steps of H radical addition are indicated by the black markers and the steps of NH_3 desorption are indicated by the red markers. CpH is first eliminated as pyridine.

The plotted reaction energies for the case that Cp is first eliminated as CpH is shown in Figure S6. We see that the computed reaction energies of CpH and NH_3 formation and desorption are all positive and the reactions are endothermic, compared to overall exothermic reactions via Cp eliminated as pyridine. We would expect that pyridine is the primary product from eliminating Cp ligand during plasma cycle.

Compared to overall endothermic reactions with the presence of Cp ligand in the elimination process, the reactions of surface NH with H radical when the Cp ligand is removed in the first step are overall exothermic. We applied Bader charge analysis to the structures formed for both the NH_2 intermediate and the ammonia by-product for the cases in which the Cp ligand is present and the Cp ligand was removed prior to formation of surface NH_x species. The results are summarized in Table 1.

Table 1. The computed charge transfer with Bader charge analysis, q(Bader) – q(valence), for the elimination of surface NH species with the presence of Cp ligand and Cp ligand removed prior to surface NH_x species.

	1st NH removal		2nd NH removal		3rd NH removal		4th NH removal	
	NH_2	NH_3	NH_2	NH_3	NH_2	NH_3	NH_2	NH_3
Cp ligand present	$0.43e^-$	$-0.08e^-$	$0.36e^-$	$-0.07e^-$	$0.35e^-$	$-0.07e^-$	$0.38e^-$	$-0.11e^-$
Cp ligand removed	$0.42e^-$	$-0.08e^-$	$0.37e^-$	$-0.05e^-$	$0.32e^-$	$-0.05e^-$	$0.35e^-$	$-0.06e^-$

For both cases, the transferred charge to intermediate NH_2 shows no differences and is in the range of $0.35e^-$ to $0.43e^-$ for each NH_2 formation step. For the ammonia formation step, if the Cp ligand is present throughout the elimination of surface NH species, there is an increasing trend of charge transfer from NH_3 to the substrate, which suggests an increasing interaction between surface Co atoms and NH_3. When the Cp ligand is removed prior to the NH species, the transferred charge from NH_3 to substrate shows a decreasing trend, which suggests a decreasing interaction between surface Co atoms and NH_3. We can infer that the computed positive reaction energies for the presence of Cp ligand in the elimination process is due to the stronger interaction (more charge transfer) between NH_3 and substrate Co atoms. Thus, the removal of the Cp ligand prior to surface NH_x species is the preferred reaction mechanism and most of the surface NH_x species will be removed with plasma-generated H radicals for lower CoCp coverage case.

3.2 Reaction of plasma radicals at Co (001) with CoCp coverage of 3.03 CoCp/nm^2

Building on the analysis of the chemistry of the plasma radicals with the low coverage of CoCp, we next examine the interaction of plasma radicals H, N, and NH with CoCp on the NH_x-

terminated Co(001) surface at the highest, stable coverage of 3.03 CoCp/nm^2.[32] In the first calculations of section 3.1, the coverages of plasma radicals are one plasma radical per CoCp fragment, so at the highest stable coverage of CoCp fragments, we consider 3H, 3N, and 3NH, respectively. These results are summarized in Table 2.

The reaction energies per plasma radical are calculated by

$$\Delta E = (E_{total} - E_{sub} - E_{n*plasma})/n \quad (3)$$

where E_{total} and E_{sub} are the energies of plasma radicals treated $(CoCp)_3NH_x$-terminated Co (001) surface the $(CoCp)_3NH_x$-terminated Co (001) surface, respectively. E_{plasma} is the total energies of plasma generated radicals, *i.e.* 3H, 3N, 3NH, and $3NH_2$ as defined above. The reference energies of these plasma radicals are indicated in section 3.1.

Table 2. Summary of reactions of surface species, *i.e.* Cp ligand and NH_x species, and plasma radicals H, N, and NH on CoCp fragments on NH_x-terminated Co(001) surface at the coverage of 3.03 CoCp/nm^2. The coverages of plasma radicals are one plasma radical per CoCp fragment, which are 3H, 3N, and 3NH. The by-products are formed spontaneously after structure relaxing.

Surface species	Plasma radicals	by-product	desorption energy per by-product/eV
3 Cp	3 H	3 CpH (C_5H_6)	1.29
	3 N	3 Pyridine (C_5H_5N)	1.17
	3 NH	3 Pyridinium (C_5H_5NH)	2.25
3 NH	3 H	3 NH_2	-
3 NH_2	3 H	3 NH_3	1.01

We first investigated the elimination of the Cp ligand via CpH formation and desorption. One hydrogen radical is placed near each Cp ring with an initial C-H distance of 1.9Å. The initial structure and relaxed stable structure are shown in Figure 4. After relaxing, 3 CpH are formed

spontaneously, with an energy change of 0.03 eV/Cp and C-H bond distance of 1.1Å. The computed energy cost per CpH for the desorption process, which results in three Co atoms deposited on the Co (001) surface, is 1.29 eV/Cp. The removal of Cp ligand for maximum three CoCp fragments on Co(001) surface via CpH formation and desorption is overall endothermic with an energy cost of 1.32 eV/Cp. This is significantly reduced compared with the energy cost of CpH formation and desorption on one CoCp fragment terminated (001) surface and indicates a cooperative role of the surface bound CoCp species in promoting ligand elimination at this higher coverage. This cooperative effect means that once sufficient numbers of precursor fragments/molecules are present on the metal surface, it can show enhanced activity for ligand exchange and desorption with lower energy cost, which is analogous to cooperative mechanism on proton transfer and ligand desorption for ALD of metal oxide such as Al_2O_3 and HfO_2.[41]

For the formation of pyridine or pyridinium cation, one N or NH radical is allowed to insert into a C=C bond in each Cp ligand. The configurations of relaxed structures are shown in Figure 5. The energy change upon N or NH insertion is -2.23eV/Cp and -2.62eV/Cp, respectively. The computed energy cost per pyridine or pyridinium for the desorption process, resulting in three Co atoms deposited on the (001) surface, are 1.17eV/pyridine and 2.25eV/pyridinium, respectively. This energy cost is reduced compared with that for the (001) surface with lower CoCp coverage. Overall, the Cp ligand elimination via pyridine or pyridinium formation and desorption are exothermic at the highest stable coverages of CoCp, whereas it is overall endothermic for Cp ligand elimination via CpH formation and desorption. Thus, the expected primary product of eliminating Cp ligand is pyridine, which is the same as the case of lower CoCp coverage.

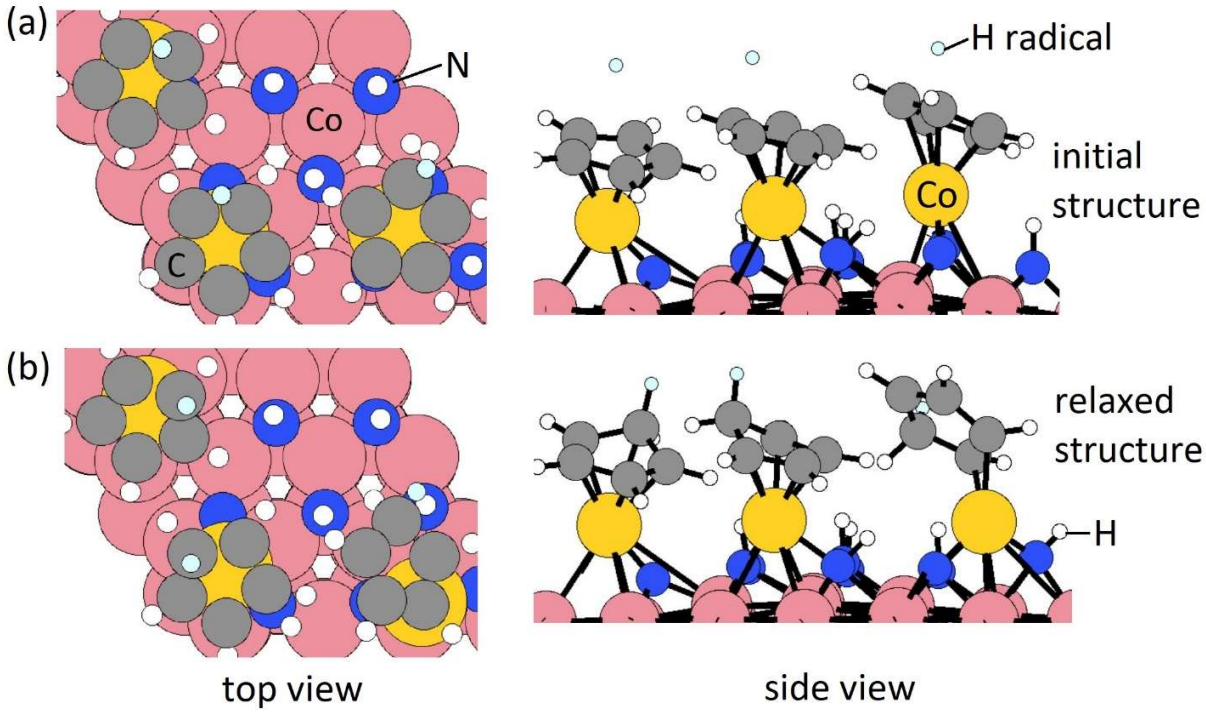

Figure 4. Configurations of top view and side view of (a) initial structure, and (b) relaxed structure for reactions of H radical and Cp ligand on NH_x-terminated Co(001) surface at the coverage of 3.03 $CoCp/nm^2$. Carbon, nitrogen, and hydrogen atoms are presented by grey, blue, and white colour. H radicals are represented by light blue sphere. Substrate Co and Co from $CoCp_2$ are represented by orange and yellow spheres, respectively.

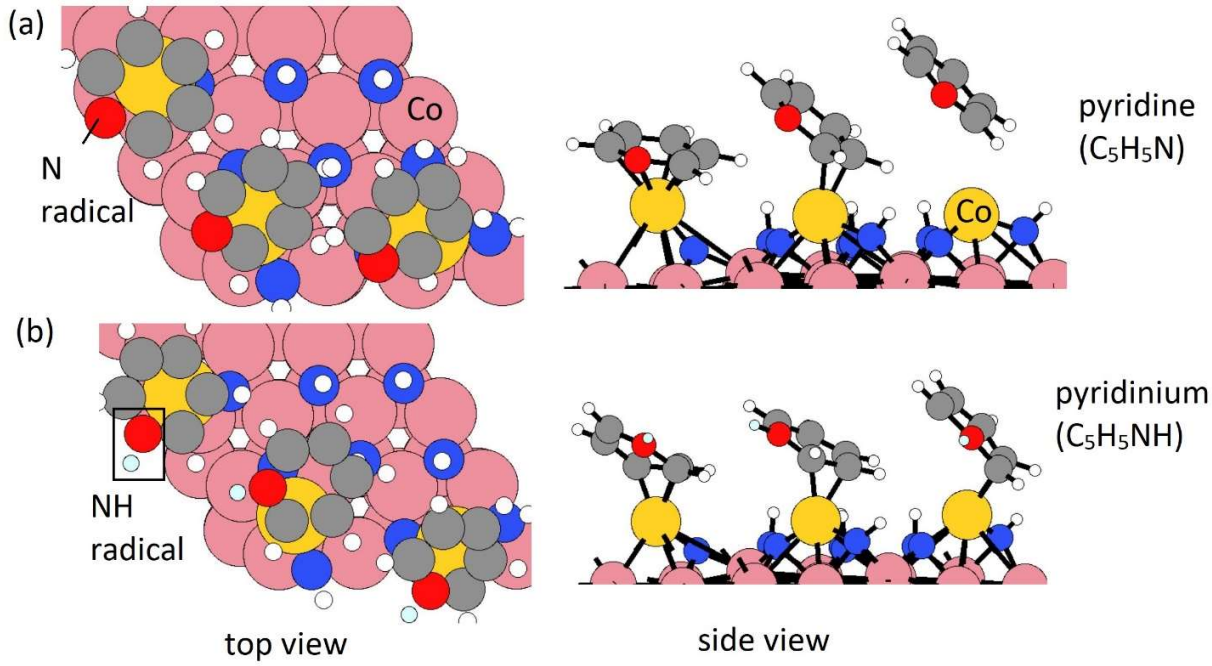

Figure 5. Configurations of top view and side view of (a) C_5H_5N, (b) C_5H_5NH for the insertion of plasma radicals N, or NH into a C=C bond of the Cp ligand on NH_x-terminated Co(001) surface at the coverage of 3.03 CoCp/nm^2. Carbon, nitrogen, and hydrogen atoms are presented by grey, blue, and white colour. Substrate Co and Co from $CoCp_2$ are represented by orange and yellow spheres, respectively. Plasma generated N and H radicals are represented by red and light blue spheres, respectively.

To investigate the interaction with the surface NH_x species, 3 H radicals are placed near three surface NH species with initial H-N distances at 1.5Å and CoCp fragments are present on the surface. The configurations of initial and relaxed stable structures of intermediate NH_2 formation are shown in Figure 6. After the formation of intermediate NH_2, with a computed negative reaction energy of -0.10eV/H and N-H bond distance of 1.0Å, 3 additional H radicals are then positioned near these surface NH_2 species. After relaxing, NH_3 forms spontaneously as shown in Figure 7, with an energy gain of -1.05eV/H. The computed energy cost per NH_3 for the desorption process is 1.01eV/NH_3, but this is more than offset by the exothermicity of the NH and NH_2 formation steps.

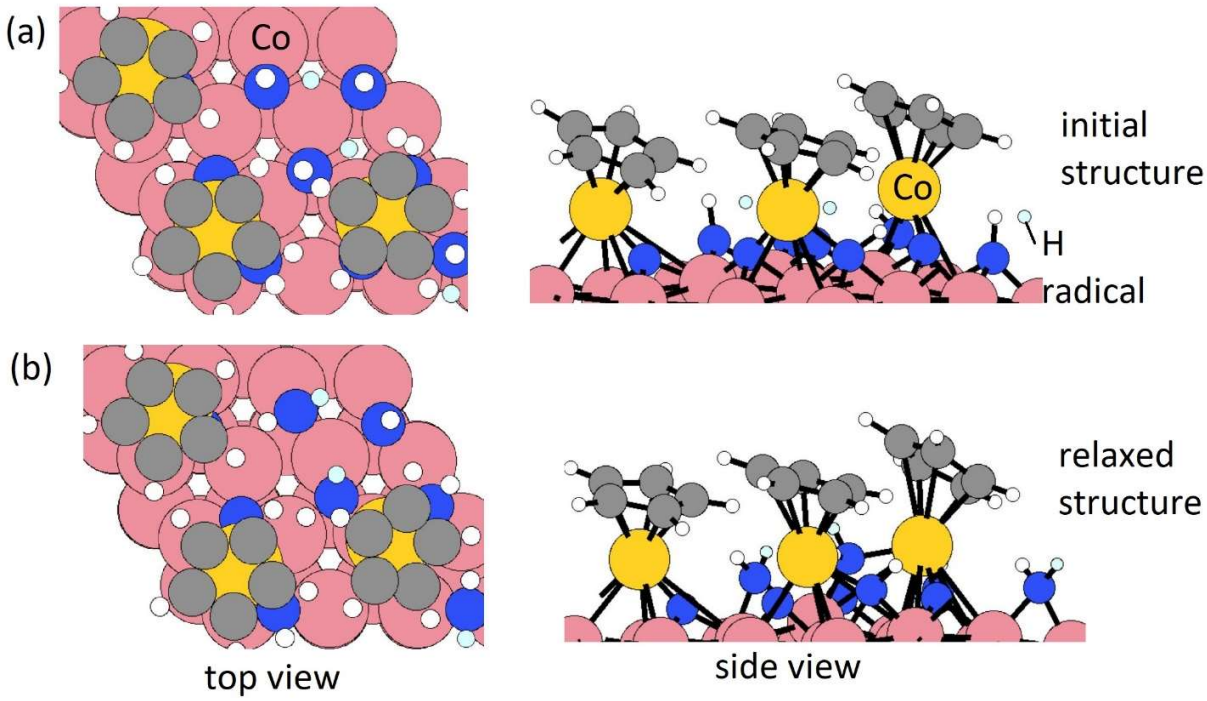

Figure 6. Configurations of top view and side view of (a) initial and (b) relaxed structure for intermediate NH_2 formation with H radical. Carbon, nitrogen, and hydrogen atoms are presented by grey, blue, and white colour. H radicals are represented by light blue sphere. Substrate Co and Co from $CoCp_2$ are represented by orange and yellow spheres, respectively.

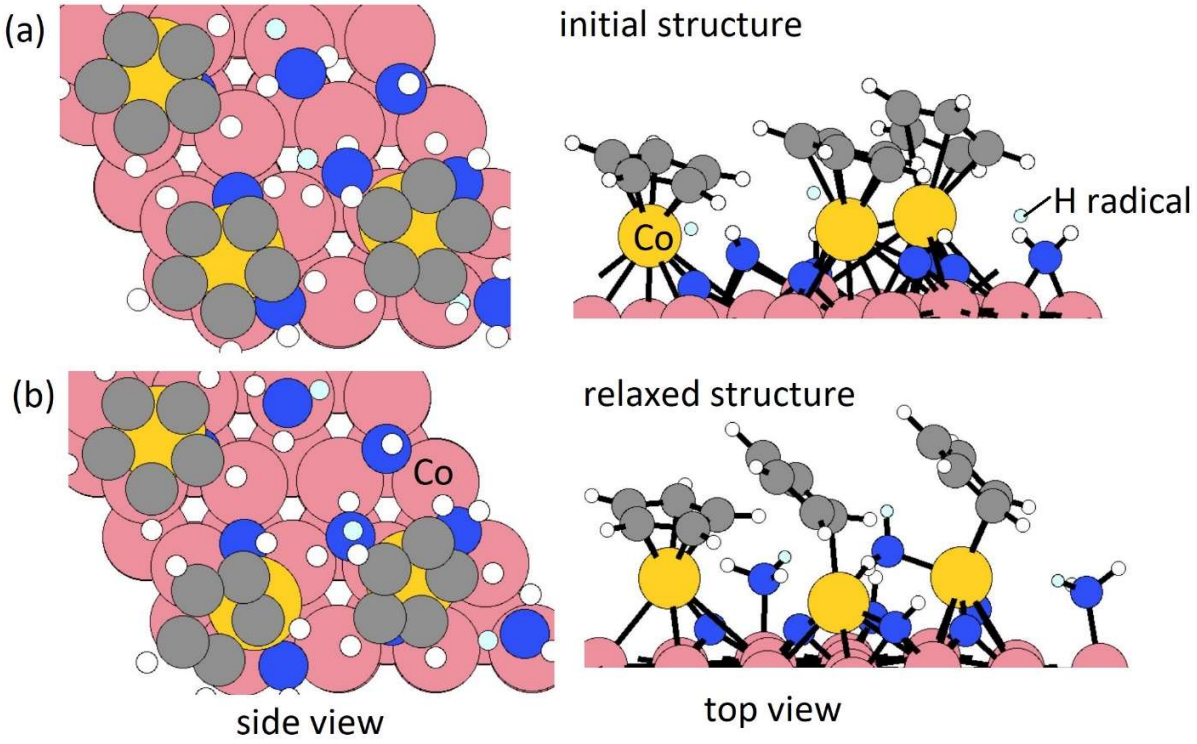

Figure 7. Configurations of top view and side view of (a) initial and (b) relaxed structure for ammonia formation with H radical and intermediate NH_2. Carbon, nitrogen, and hydrogen atoms are presented by grey, blue, and white colour. H radicals are represented by light blue sphere. Substrate Co and Co from $CoCp_2$ are represented by orange and yellow spheres, respectively.

We now consider the elimination of NH_x on Co(001) surface terminated with 3CoCp using H radicals, in which the Cp ligand was removed in the first step via pyridine formation and desorption. The reaction energies are computed using equation (2) in section 3.1.

The computed reaction energies for initial Cp ligand removal and subsequent ammonia formation are all negative on 3CoCp-terminated Co(001) surface. A cooperative effect of the surface-bound CoCp fragments is observed when compared to single CoCp fragment, which makes the removal of Cp ligand exothermic and favourable on the surface with the higher CoCp-coverages. For the

removal of surface NH species, the determined preferred pathway is an exothermic NH ≫ NH_2 ≫ NH_3. After the Cp ligand and NH_x species are removed completely, three Co atoms are deposited on the Co(001) surface, with a computed exothermic reaction energy of -4.85eV. The plotted reaction pathway and configurations of structures along the pathway are shown in Figure 8 and Figure S7, respectively.

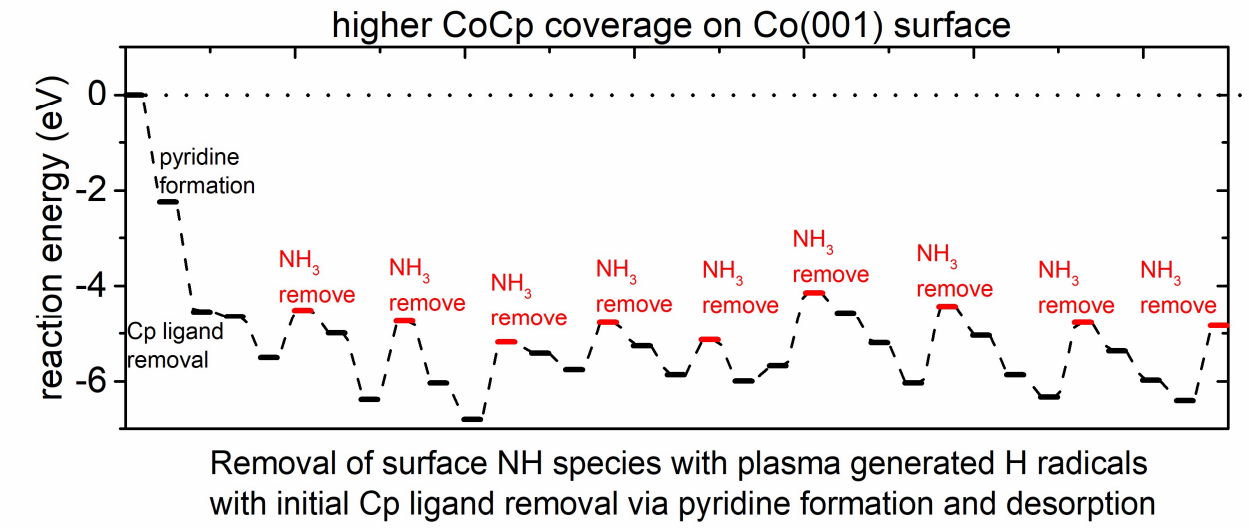

Figure 8. The plotted reaction pathway for removal of surface NH species with plasma generated H radicals with initial Cp ligand removed on 3CoCp-terminated Co(001) surface. The steps of H radical addition are indicated by the black markers and the steps of NH_3 desorption are indicated by the red markers.The Cp ligand is first eliminated as pyridine.

The plotted reaction energies for the case that Cp is first eliminated as CpH is shown in Figure S8. We see that the computed reaction energies of CpH and NH_3 formation and desorption are all positive and the reactions are endothermic, compared to overall exothermic reactions via Cp eliminated as pyridine. We would expect that pyridine is a primary product from eliminating Cp ligand during plasma cycle.

To summarize, these T = 0 K results indicate that the N radical plays an important role in eliminating Cp ligands present on the surface (if any) via pyridine formation and desorption and H radicals contribute to the elimination of surface NH_x species via NH_3 formation and desorption.

The elimination process of surface NH species is exothermic when using H radicals. NH species are removed via intermediate NH_2 formation, by-product NH_3 formation and desorption. Surface N species, resulting from H transfer to Cp ligand on metal precursor pulse, are also removed via NH, NH_2 formation, and release of NH_3. The surface NH_x species are completely eliminated with plasma generated H radicals, resulting in deposition of Co atoms on the Co(001) surface at a coverage of 3.03 Co/nm^2.

3.3 Reactions of plasma generated H radicals on NH_x-terminated Co(100) surface

After metal precursor ($CoCp_2$) pulse, the higher energy Co (100) surface is terminated with Co atoms at a coverage of 3.33 Co/nm^2. From our previous study[32] on the mechanism of metal precursor pulse, the trench NH species are involved in the H transfer to eliminate Cp ligand as CpH. The surface NH_2 species have endothermic reaction energies for CpH elimination. Thus, after the metal precursor pulse in a (3×3) supercell we have three deposited Co atoms with six surface NH_2 and six trench N atoms that have lost H atoms in the metal precursor step.

During the plasma step, these remaining NH_x species may be eliminated by the reaction with plasma generated radicals H, N, NH, and NH_2 via NH_3, N_2H_2, or N_2H_4 formation and desorption, analogous to the removal of surface NH_x species on the Co(001) surface. We first performed calculations for reactions of eliminating surface NH_2 species with H radicals via NH_3 formation and desorption. H radicals are placed near surface NH_2 with an initial N-H distance at 1.5Å and

examine successive interactions of surface NH_2. The plotted energy pathway for ammonia formation and desorption is shown in Figure 9. The reaction energies are calculated using the equation (2) described in section 3.1. The configurations of structures along the reaction pathway is shown in Figure S9. While ammonia is formed spontaneously after relaxing the structure, the computed reaction energies are all positive, indicating endothermic reactions for removal of surface NH_2 species with H radicals. The energy cost of NH_3 desorption on Co(100) surface is around 1.2eV at each desorption step. After the desorption of the 6th NH_3, the overall reaction energy is as high as 5.80eV. This indicates that on NH_x-terminated Co(100) surface, the surface NH_2 species cannot be completely eliminated by H radicals.

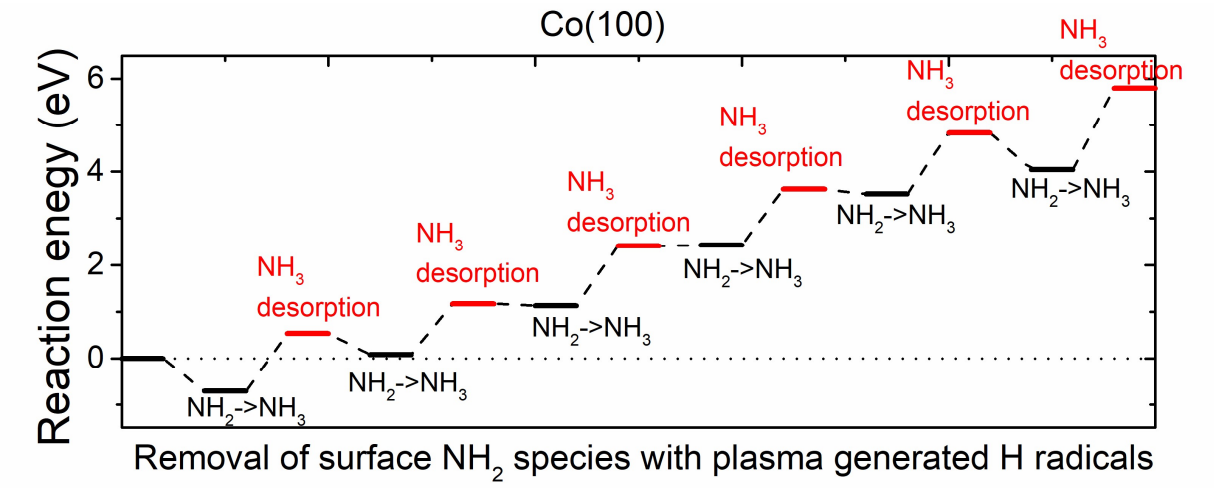

Figure 9. The plotted reaction pathway for removal of surface NH_2 species with plasma generated H radicals on NH_x-terminated Co(100) surface.

We then performed calculations for reactions of trench N species and H radicals. The results show that trench N species can react with H radicals to form NH, with a computed reaction energy of 0.24eV for the 1st NH formation. However, there are no further reactions to form intermediate NH_2 or by-product NH_3. Instead, the next H radicals prefer to react with another trench N species to form NH. The plotted reaction pathway for trench NH formation is shown in Figure 10. The

computed reaction energies are overall negative, except for a small energy cost for the formation of the first NH. The configurations of structures along the reaction pathway are shown in Figure S10. We note that for the 6th H radical, it would prefer to bind to surface Co atoms rather than recover the 6th N to NH species. Thus, for trench N species, at the plasma step with H radicals, at most five N species can recover to NH. These results indicate the difficulty in eliminating N species from the Co (100) surface via ammonia formation.

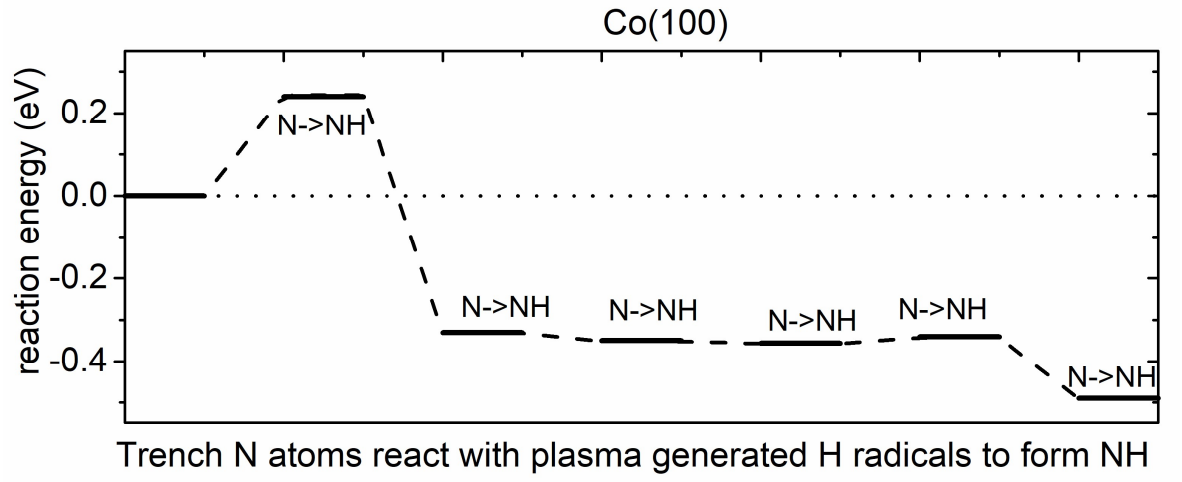

Figure 10. The plotted reaction pathway for trench N atoms recover to NH with plasma generated H radicals on NH_x-terminated Co(100) surface.

Given the difficulty in eliminating surface NH_2 and trench N via NH_3 formation and desorption, we have computed the reaction energies for the formation of hydrazine (N_2H_4) and diazene (N_2H_2) that are formed through the interaction with NH and NH_2 radicals. After static DFT relaxations, hydrazine or diazene dissociate into two NH_2 or two NH that are bound to the Co (100) surface, indicating the unfavourable formation of hydrazine and diazene.

To summarise, on the Co(100) surface, the removal of surface NH_x species as ammonia is endothermic, while it is an exothermic reaction on the Co(001) surface. Instead, on Co(100),

plasma generated H radicals react with trench N species to form stable NH species, which are then available for the next hydrogen transfer step in the next metal precursor pulse.

3.4 Ab initio molecular dynamics simulations of the reaction of plasma radicals at Co (001) and (100) surfaces

On Co(001) surface, *ab initio* molecular dynamics (AIMD) calculations were performed by introducing 9 H radicals at a temperature of 600K. We form pyridine through N radical insertion, at a coverage of 3.03 pyridine/nm^2. The time step is 1.5fs, with total running time at 2.25ps with the NVT (canonical) ensemble. The structures at the end of the MD simulations are shown in Figure 11 and a movie of the simulation is shown in the supporting information. Over half of H radicals recombine to form H_2 molecules, which is first observed at 0.21 ps (Fig. S11(a)). Some H radicals contribute to NH_3 formation at 0.33 ps (Fig.S11 (b)) and pyridinium formation at 1.26 ps (Fig. S11(c)). Thus, upon introducing 9 H radicals on Co(001) surface with surface bound pyridine at a coverage of 3.03 pyridine/nm^2, the MD results indicate that surface NH_x species can be eliminated via NH_3 formation and desorption while surface bound pyridine is eliminated via either direct desorption or pyridinium formation and desorption. These results are consistent with the static DFT calculations in section 3.1 and 3.2.

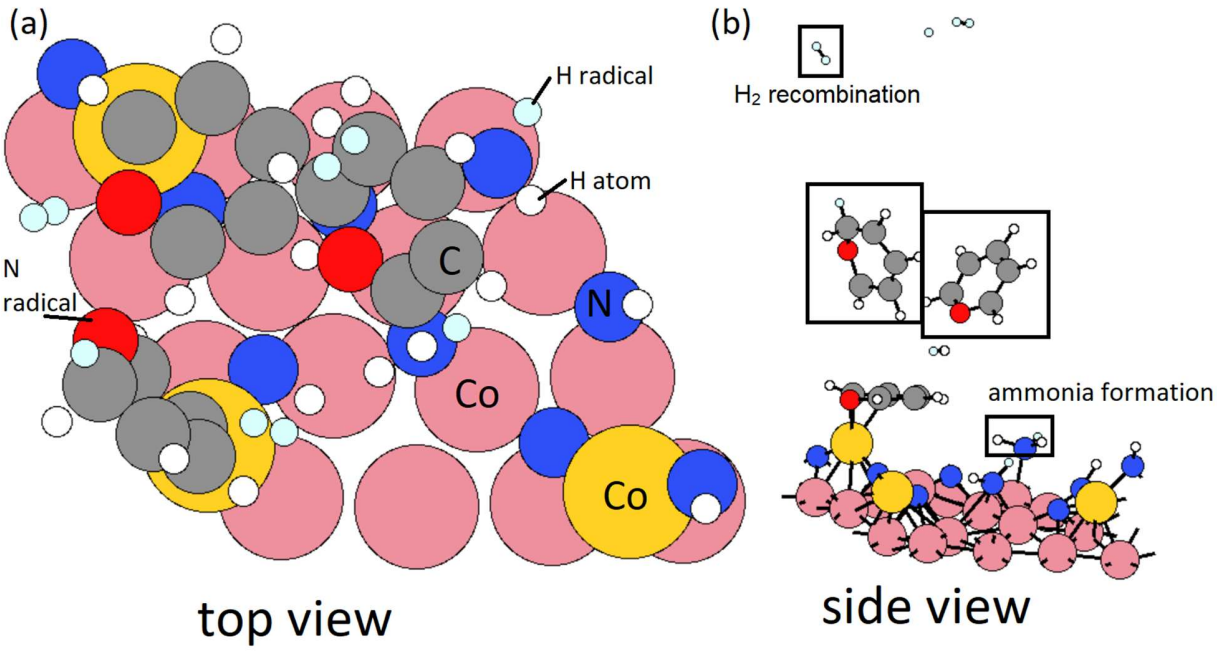

Figure 11. The structure snapshot at the end of the MD calculation at 600K on the NH_x-terminated Co(001) surface with 9 H radicals in (a) top view, and (b) side view. Carbon, nitrogen, and hydrogen atoms are presented by grey, blue, and white colour. H radicals are represented by light blue sphere. Substrate Co and Co from $CoCp_2$ are represented by orange and yellow spheres, respectively. H and N radicals are represented by light blue and red spheres, respectively.

To explore the dynamics on the Co(100) surface, MD calculations are performed on the NH_x-terminated Co(100) surface with six deposited Co atoms on the surface at temperatures of 600K and 1000K. The time step is 1.5fs with total simulation time of 2.25ps with the NVT ensemble. The structures at the end of this MD simulation are shown in Figure 12. For T=600K and 1000K, there is no desorption of surface NH_x terminations indicating that the removal of these surface bound NH_x species requires a high energy cost. This is in line with the static DFT results of computed endothermic reactions of eliminating surface NH_x species with H radicals. For T=1000K, we see that the deposited surface Co atoms migrates to form small Co nanoclusters due to trench N migrating to surface sites.

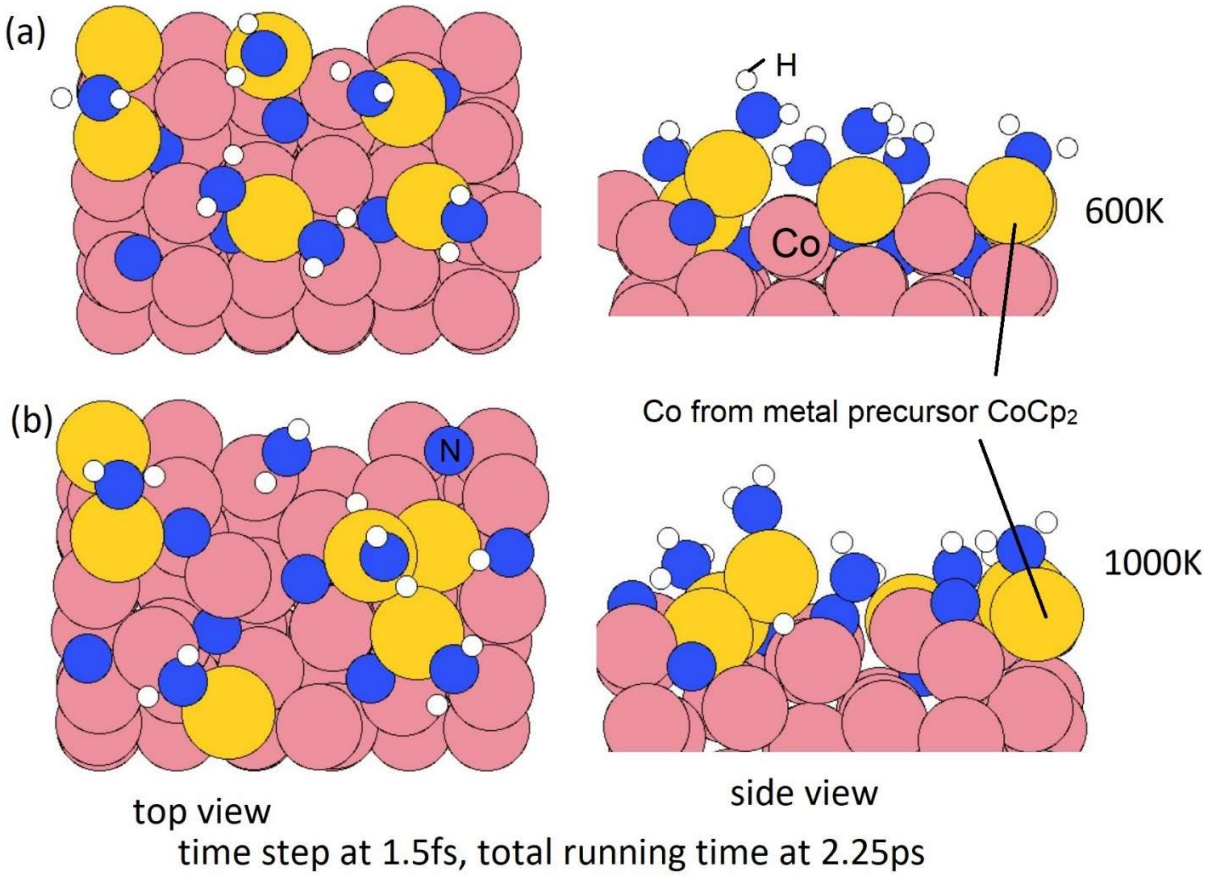

Figure 12. The configurations of resulting structures after MD calculations at (a) 600K, and (b) 1000K on NH_x-terminated Co(100) surface with six deposited Co atoms on the surface. Carbon, nitrogen, and hydrogen atoms are presented by grey, blue, and white colour. Substrate Co and Co from $CoCp_2$ are represented by orange and red spheres, respectively.

4. Discussion

4.1 Structures of N-plasma treated Co (001) and (100) surfaces

On the low energy Co(001) surface, during the plasma cycle the Cp ligand and surface NH_x species are eliminated by plasma generated N and H radicals, resulting in Co atoms deposited on the Co(001) surface at a coverage of 3.03 Co/nm^2. On the Co(100) surface, the surface NH_2 species cannot be eliminated with H radicals since these reactions are endothermic. The trench N species

will transform to NH after interaction with H radicals. These trench N species on Co(100) surface will be a potential source of N impurities in deposited Co thin films.[30, 42]

We applied Bader charge analysis to the Co (001) and (100) surfaces in each step of NH_x removal. The results are summarized in Table 3. On the Co(001) surface, the Cp ligands have been removed prior to the interaction of surface NH species with N radicals. The computed transferred charges for the formation of the ammonia by-product are almost the same at a value of *ca.* -0.10e^- on NH_x-terminated Co(001) surface. However, on NH_x-terminated Co(100) surface, the computed transferred charge from NH_3 to substrate Co atoms at NH_3 formation step increase from 0.06e^- to 0.13e^- along the elimination pathway. This indicates the interaction between NH_3 and substrate Co atoms becomes stronger along the elimination pathway on Co(100) surface, which is in accordance with the computed positive reaction energies for NH_3 formation and desorption on (100) surface.

Table 3. The computed charge transfer with Bader charge analysis, q(Bader) – q(valence), for the elimination of surface NH_x species on 3CoCp fragments terminated Co(001) surface and NH_x-terminated Co(100) surface. Noted that the Cp ligands are eliminated prior to surface NH species on Co(001) surface.

	1st NH_x removal	2nd NH_x removal	3rd NH_x removal	4th NH_x removal	5th NH_x removal	6th NH_x removal	7th NH_x removal	8th NH_x removal	9th NH_x removal
	NH_3	NH_3	NH_3	NH_3	NH_3	NH_3	NH_3	NH_3	NH_3
Co(001)	-0.08e^-	-0.11e^-	-0.10e^-	-0.09e^-	-0.10e^-	-0.10e^-	-0.07e^-	-0.08e^-	-0.08e^-
Co(100)	-0.05e^-	-0.06e^-	-0.06e^-	-0.08e^-	-0.11e^-	-0.13e^-	-	-	-

On Co(001) surface, after few cycles, a full layer Co atoms will be deposited on the surface and surface NH_x species are completely removed at the plasma cycle. Whereas, on Co(100) surface, the NH_x species cannot be completely eliminated. We have examined a full layer of Co atoms

(1ML, in total 9 Co atoms) deposited on the Co(100) surface and this is shown in Figure 13(a). The initial surface Co atoms become trench Co atoms and the deposited Co atoms become new surface Co atoms. From our previous thermodynamics study on NH_x-terminated Co surfaces, NH_2 prefers surface bridge site and NH prefers trench bridge site.[31] With this in mind, we have performed calculations of surface rearrangement on NH_x-terminated Co(100) surface with a full layer of deposited Co atoms. The relaxed structure is shown in Figure 13(b). This surface NH_x rearrangement is exothermic with a negative energy gain at the value of -0.48eV. After rearrangement, NH_2 binds to surface bridge sites.

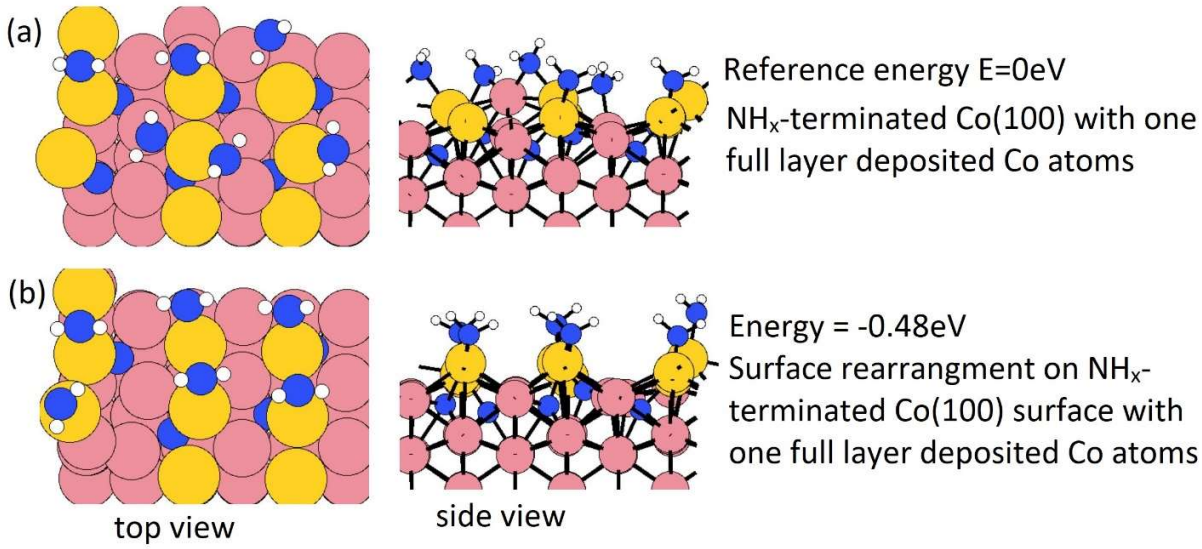

Figure 13. The top view and side view of (a) relaxed original structure, and (b) structure after surface NH_x rearrangement on NH_x-terminated Co(100) with one full layer deposited Co atoms. Carbon, nitrogen, and hydrogen atoms are presented by grey, blue, and white colour. Substrate Co and Co from $CoCp_2$ are represented by orange and red spheres, respectively.

4.2 Regeneration of surface NH_x Terminations

If we consider the next ALD cycle, at the post-plasma stage, the metal surface is supposed to be terminated with NH_x species before the next metal precursor half-reaction, analogous to the regeneration of hydroxyl groups in thermal or plasma assisted metal oxide ALD.[43-44] To explore how this surface can form, we have performed MD calculations at 600K for the interaction of NH radicals with the Co(001) surface, where Co atoms were deposited at a coverage of 3.03 Co/nm^2 and the original surface NH species were eliminated as ammonia. Two coverages of NH radicals are explored, *i.e.* 0.67ML (in total 6NH) and 0.89ML (in total 8 NH) on (3×3) supercell (1ML corresponds to 9 NH radicals). The time step is 1.5fs with a simulation time of 2.25ps in the NVT ensemble. The structures at the two coverages of NH radicals after MD calculations are shown in Figure 14.

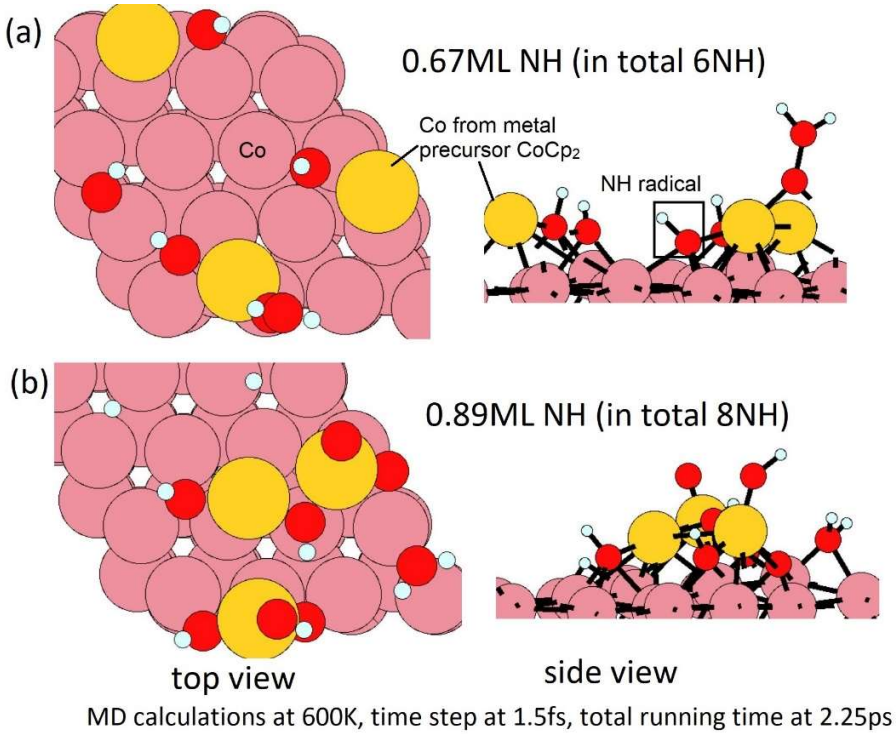

Figure 14. The configurations of structures after MD calculations on Co(001) surface with NH radicals at the coverage of (a) 0.67ML, and (b) 0.89ML. Carbon, nitrogen, and hydrogen atoms are presented by grey, blue, and white colour. Substrate Co and Co from $CoCp_2$ are represented by orange and yellow spheres, respectively. Plasma generated N and H radicals are represented red and light blue spheres, respectively.

From these simulations, the Co(001) surface is covered with NH terminations at a coverage of 0.44ML (4NH on the surface). This coverage is slightly lower than the determined stable coverage of NH terminations on Co (001) surface from our previous study[31], which is 0.56ML (5NH on the surface). At an initial higher coverage of 0.89ML NH, we observe formation of surface bound NH and NH_2 species, as well as surface bound H species and N species, which form as a result of the dissociation of NH radicals under these simulation conditions. We can infer that at the post-plasma stage, NH radicals contribute to the formation of the NH_x-terminations on the metal surface, which then contributes in the Cp ligand elimination in the next metal precursor pulse. Hydrogen alone cannot produce the reactive NH species; although N_2 alone would promote Cp ligand elimination via pyridine formation, these N radicals cannot produce reactive NH surface termination. Thus, the plasma deposition of Co requires both hydrogen and nitrogen/ammonia plasma.

Then, we perform MD calculations at 600K to explore how NH_x-terminations are formed on Co(100) surface at the post-plasma stage. The Co(100) surface after NH_x rearrangement (Figure 14(b)) is chosen to be the substrate. The coverage of NH radicals is 0.67ML (in total 6 NH), which are previously determined as the saturation coverage of trench NH species at ALD deposition temperature.[31] The time step is 1.5fs with a simulation time of 2.25ps with the NVT (or canonical) ensemble. The initial structure and final structure are shown in Figure 15. By-products NH_3 and N_2 are formed and released, resulting in surface terminations including surface bound N, surface bound NH_2, and trench NH species. The original trench N atoms are now incorporated into the subsurface layer. One full layer of Co atoms is deposited and the terminations after the post-plasma stage are NH_x-terminations with $4NH_2$ + 4NH on Co(100) surface. This coverage is slightly lower

than the determined stable coverage of mixed terminations on Co (100) surface from our previous study[31], which is 6NH + 6NH_2 on the surface.

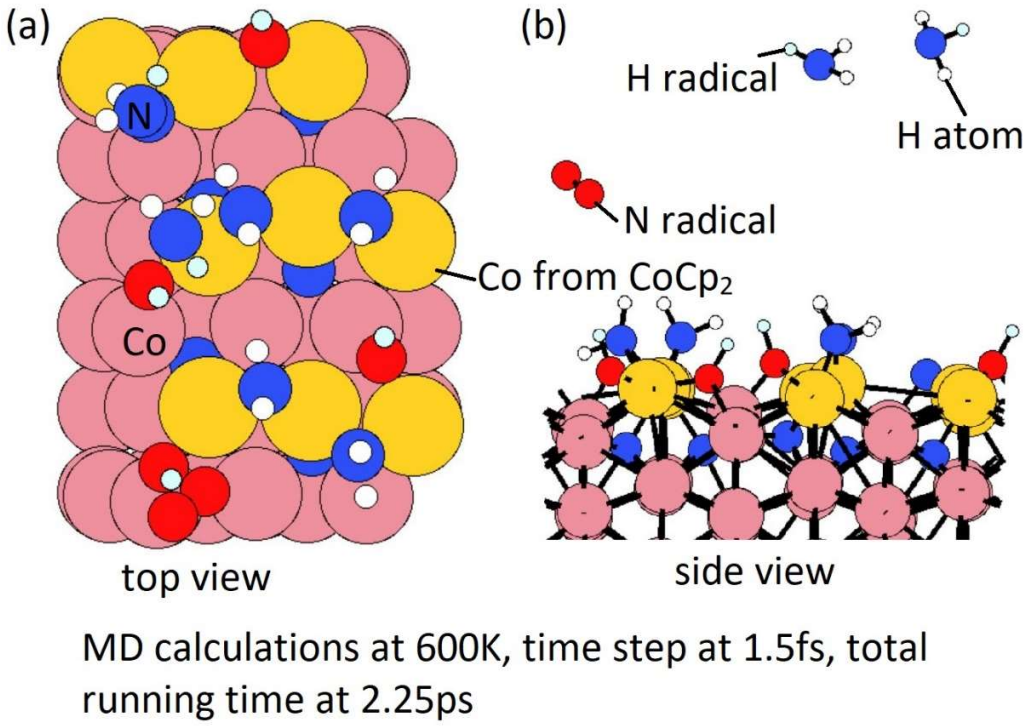

Figure 15. The configurations of (a) initial structure, and (b) final structure for MD calculations on the structure after surface rearrangement and NH radicals. Carbon, nitrogen, and hydrogen atoms are presented by grey, blue, and white colour. Substrate Co and Co from $CoCp_2$ are represented by orange and yellow spheres, respectively. Plasma generated N and H radicals are represented red and light blue spheres, respectively.

It is noted that the trench N species are present throughout the deposition process and cannot be removed completely in either the metal precursor or plasma cycle. We can infer that the N impurities exists with the possibility of formation of Co_xN. This is consistent with the reported nitrogen incorporation into deposited Co thin films and Cobalt nitride using $CoCp_2$ and NH_3 plasma.[30, 42] At temperatures of 533K and below, the deposited thin films consist primarily of Co_2N. At higher temperature at 573K, the Co_xN is a mixture of Co_3N and Co. Finally, if the

temperature is up to 623K, the deposited thin film is nominally pure Co, which is due to the decomposition of Cobalt nitride.[30] Detailed studies are needed to study the formation of surface cobalt nitride and removal of these N species, which is out of the scope of current paper.

5. Conclusions

We have presented a detailed first principles study of the chemistry of the plasma pulse in hydrogen/nitrogen plasma enhanced ALD of Co metal. We begin with a surface after the metal precursor pulse, with CoCp fragment terminated Co (001) surface at a coverage of 3.03CoCp/nm^2 and an NH_x-terminated Co (100) surface with deposited Co atoms at a coverage of 3.33Co/nm^2. This work focuses on the reaction mechanism in plasma cycle of plasma radicals and Co (001) and (100) surfaces terminated with Cp ligand (if any) and NH_x species in atomic scale.

On Co(001) surface, the preferred reaction mechanism is that Cp ligand is eliminated prior to surface NH_x species via pyridine formation and desorption with plasma generated N radicals. Bader charge analysis indicates that for the ammonia desorption step, Cp ligand eliminated prior to NH_x elimination has less transferred charge between NH_3 and substrate Co, compared to Cp ligand present throughout. The surface NH species and N species are eliminated via intermedia NH formation, NH_2 formation, by-product NH_3 formation and desorption. The reactions of Cp ligand removal and subsequent NH_x removal are overall exothermic, which are completely eliminated on Co(001) surface, resulting deposited Co atoms on (001) surface at a coverage of 3.03 Co/nm^2.

There is a different behaviour on the Co(100) surface. The surface NH_2 species cannot be completely removed with H radicals via NH_3 formation and desorption due to an overall endothermic reaction emergy. Instead, H radicals will contribute to reform trench NH species with

computed negative reaction energies. When a full layer of Co atoms are deposited on Co(100) surface, due to its unique zigzag structure, the original surface Co atoms become trench Co and the deposited Co atoms occupy the surface site. However, these trench N species are present throughout the deposition process and result in formation of Co_xN and cannot be removed completely at the conditions of our simulations. This indicates the plasma species acting as the sources of N impurities in deposited Co thin films.

At the post-plasma stage, MD simulations at 600K shows that NH radicals play an important role in regenerations of NH_x-terminations on Co (001) and (100) surfaces, which is then ready for the next metal precursor half-cycle. For Cp-based metal precursors, NH_x species are required to deposit Co thin film with high purity and low resistivity, which explains why NH_3 plasma or a mixture of N_2 and H_2 plasma are the plasma sources that work best, rather than H_2 plasma or N_2 plasma alone.

Acknowledgements

We acknowledge generous support from Science Foundation Ireland (SFI) through the SFI-NSFC Partnership program, Grant Number 17/NSFC/5279, NITRALD and National Natural Science Foundation of China, Grant number 51861135105. Computing resources have been generously supported by Science Foundation Ireland at Tyndall and through the SFI/HEA-funded Irish Centre for High End Computing (www.ichec.ie). J.L. acknowledges that part of the results of this research have been achieved using the DECI resource BEM cluster based in Poland at Wroclaw Centre for Networking and Supercomputing with support from the PRACE.

References

1. Tu, K., Recent Advances on Electromigration in Very-Large-Scale-Integration of Interconnects. *J. Appl. Phys.* **2003,** *94*, 5451-5473.

2. Kondati Natarajan, S.; Nies, C.-L.; Nolan, M., Ru passivated and Ru doped ε-TaN surfaces as a combined barrier and liner material for copper interconnects: a first principles study. *J. Mater. Chem. C* **2019,** *7* (26), 7959-7973.
3. Greenslit, D. V.; Eisenbraun, E., Characterization of Ultrathin PEALD-Grown RuCo Films for Diffusion Barrier and Copper Direct-Plate Applications. *ECS Trans.* **2011,** *35*, 17-24.
4. Chakraborty, T.; Eisenbraun, E. T., Microstructure Analysis of Plasma Enhanced Atomic Layer Deposition-Grown Mixed-Phase RuTaN Barrier for Seedless Copper Electrodeposition. *J. Vac. Sci. Technol. A* **2012,** *30*, 020604 1-5.
5. Miikkulainen, V.; Leskelä, M.; Ritala, M.; Puurunen, R. L., Crystallinity of Inorganic Films Grown by Atomic Layer Deposition: Overview and General Trends. *J. Appl. Phys.* **2013,** *113*, 021301 1-101.
6. Johnson, R. W.; Hultqvist, A.; Bent, S. F., A Brief Review of Atomic Layer Deposition: From Fundamentals to Applications. *Mater. Today* **2014,** *17*, 236-246.
7. Kaloyeros, A. E.; Pan, Y.; Goff, J.; Arkles, B., Review—Cobalt Thin Films: Trends in Processing Technologies and Emerging Applications. *ECS J. Solid State Sci.* **2019,** *8*, P119-P152.
8. George, S. M., Atomic Layer Deposition: An Overview. *Chem. Rev.* **2009,** *110*, 111-131.
9. Profijt, H.; Potts, S.; Van de Sanden, M.; Kessels, W., Plasma-Assisted Atomic Layer Deposition: Basics, Opportunities, and Challenges. *J. Vac. Sci. Technol. A* **2011,** *29*, 050801 1-26.
10. Oviroh, P. O.; Akbarzadeh, R.; Pan, D.; Coetzee, R. A. M.; Jen, T. C., New Development of Atomic Layer Deposition: Processes, Methods and Applications. *Sci. Technol. Adv. Mater.* **2019,** *20*, 465-496.
11. Kim, H., Atomic Layer Deposition of Mmetal and Nitride Thin Films: Current Research Efforts and Applications for Semiconductor Device Processing. *J. Vac. Sci. Technol. B* **2003,** *21*, 2231-2261.
12. Knisley, T. J.; Kalutarage, L. C.; Winter, C. H., Precursors and Chemistry for The Atomic Layer Deposition of Metallic First Row Transition Metal Films. *Coordin. Chem. Rev.* **2013,** *257*, 3222-3231.
13. Kim, H., Area Selective Atomic Layer Deposition of Cobalt Thin Films. *ECS Trans.* **2008,** *16*, 219-225.
14. Lim, B. S.; Rahtu, A.; Gordon, R. G., Atomic Layer Deposition of Transition Metals. *Nat. Mater.* **2003,** *2*, 749-754.
15. Kim, J.-M.; Lansalot, C.; Dussarrat, C.; Gatineau, J.; Kim, H., Plasma-enhanced atomic layer deposition of cobalt using cyclopentadienyl isopropyl acetamidinato-cobalt as a precursor. *Jpn. J. Appl. Phys* **2010,** *49*, 05FA10.
16. Kim, K.; Lee, K.; Han, S.; Jeong, W.; Jeon, H., Characteristics of Cobalt Thin Films Deposited by Remote Plasma ALD Method with Dicobalt Octacarbonyl. *J. Electrochem. Soc.* **2007,** *154*, H177-H181.
17. Kim, H., High-Quality Cobalt Thin Films by Plasma-Enhanced Atomic Layer Deposition. *Electrochem. Solid-State Lett.* **2006,** *9*, G323-G325.
18. Puurunen, R. L., Surface Chemistry of Atomic Layer Deposition: A Case Study for The Trimethylaluminum/Water Process. *J. Appl. Phys.* **2005,** *97*, 121301 1-52.
19. Elliott, S.; Scarel, G.; Wiemer, C.; Fanciulli, M.; Pavia, G., Ozone-Based Atomic Layer Deposition of Alumina from TMA: Growth, Morphology, and Reaction Mechanism. *Chem. Mater.* **2006,** *18*, 3764-3773.
20. Weckman, T.; Laasonen, K., First Principles Study of The Atomic Layer Deposition of Alumina by TMA–H_2O-Process. *Phys. Chem. Chem. Phys.* **2015,** *17*, 17322-17334.
21. Weckman, T.; Laasonen, K., Atomic Layer Deposition of Zinc Oxide: Diethyl Zinc Reactions and Surface Saturation from First-Principles. *J. Phys. Chem. C* **2016,** *120* (38), 21460-21471.
22. Lee, S.-J.; Kim, S.-H.; Saito, M.; Suzuki, K.; Nabeya, S.; Lee, J.; Kim, S.; Yeom, S.; Lee, D.-J., Plasma-Free Atomic Layer Deposition of Ru Thin Films Using H_2 Molecules as A Nonoxidizing Reactant. *J. Vac. Sci. Technol. A* **2016,** *34* (3), 031509.
23. Zhu, B.; Ding, Z.-J.; Wu, X.; Liu, W.-J.; Zhang, D. W.; Ding, S.-J., Plasma-Enhanced Atomic Layer Deposition of Cobalt Films Using $Co(EtCp)_2$ as A Metal Precursor. *Nanoscale Res. Lett.* **2019,** *14*, 76 1-7.

24. Kim, H.; Oh, I.-K., Review of plasma-enhanced atomic layer deposition: Technical enabler of nanoscale device fabrication. *Jpn. J. Appl. Phys* **2014,** *53* (3S2), 03DA01.
25. Rossnagel, S.; Sherman, A.; Turner, F., Plasma-enhanced atomic layer deposition of Ta and Ti for interconnect diffusion barriers. *J. Vac. Sci. Technol. B* **2000,** *18*, 2016-2020.
26. Yoon, J.; Kim, D.; Cheon, T.; Kim, S.-H.; Kim, H., Atomic Layer Deposition of Co Using N_2/H_2 Plasma as A Reactant. *J. Electrochem. Soc.* **2011,** *158*, H1179-H1182.
27. Vos, M. F.; van Straaten, G.; Kessels, W. E.; Mackus, A. J., Atomic Layer Deposition of Cobalt Using H_2-, N_2-, and NH_3-Based Plasmas: On the Role of the Co-reactant. *J. Phys. Chem. C* **2018,** *122*, 22519-22529.
28. Nolan, M.; Elliott, S. D., Competing Mechanisms in Atomic Layer Deposition of Er_2O_3 versus La_2O_3 from Cyclopentadienyl Precursors. *Chem. Mater.* **2010,** *22*, 117-129.
29. Rai, V. R.; Vandalon, V.; Agarwal, S., Surface Reaction Mechanisms During Ozone and Oxygen Plasma Assisted Atomic Layer Deposition of Aluminum Oxide. *Langmuir* **2010,** *26*, 13732-13735.
30. van Straaten, G.; Deckers, R.; Vos, M. F.; Kessels, W. M.; Creatore, M., Plasma-Enhanced Atomic Layer Deposition of Cobalt and Cobalt Nitride: What Controls the Incorporation of Nitrogen? *J. Phys. Chem. C* . **2020,** *124*, 22046-22054.
31. Liu, J.; Nolan, M., Coverage and Stability of NHx-Terminated Cobalt and Ruthenium Surfaces: A First-Principles Investigation. *J. Phys. Chem. C* **2019,** *123*, 25166-25175.
32. Liu, J.; Lu, H.; Zhang, D. W.; Nolan, M., Reaction Mechanism of the Metal Precursor Pulse in Plasma-Enhanced Atomic Layer Deposition of Cobalt and the Role of Surface Facets. *The Journal of Physical Chemistry C* **2020,** *124* (J. Phys. Chem. C), 11990-12000.
33. Kresse, G.; Joubert, D., From Ultrasoft Pseudopotentials to The Projector Augmented-wave Method. *Phys. Rev. B* **1999,** *59*, 1758-1775.
34. Kresse, G.; Hafner, J., Ab initio molecular-dynamics simulation of the liquid-metal–amorphous-semiconductor transition in germanium. *Phys. Rev. B* **1994,** *49*, 14251.
35. Perdew, J. P.; Chevary, J. A.; Vosko, S. H.; Jackson, K. A.; Pederson, M. R.; Singh, D. J.; Fiolhais, C., Atoms, Molecules, Solids, and Surfaces: Applications of The Generalized Gradient Approximation for Exchange and Correlation. *Phys. Rev. B* **1992,** *46*, 6671-6687.
36. Perdew, J. P.; Burke, K.; Ernzerhof, M., Generalized Gradient Approximation Made Simple. *Phys. Rev. Lett.* **1996,** *77*, 3865-3868.
37. Monkhorst, H. J.; Pack, J. D., Special Points for Brillouin-zone Integrations. *Phys. Rev. B* **1976,** *13*, 5188-5192.
38. Maimaiti, Y.; Elliott, S. D., Precursor Adsorption on Copper Surfaces as the First Step during the Deposition of Copper: A Density Functional Study with van der Waals Correction. *J. Phys. Chem. C* **2015,** *119*, 9375-9385.
39. Yu, M.; Trinkle, D. R., Accurate and efficient algorithm for Bader charge integration. *J. Chem. Phys.* **2011,** *134*, 064111.
40. Tang, W.; Sanville, E.; Henkelman, G., A grid-based Bader analysis algorithm without lattice bias. *J. Condens. Matter Phys.* **2009,** *21*, 084204.
41. Shirazi, M.; Elliott, S. D., Cooperation between adsorbates accounts for the activation of atomic layer deposition reactions. *Nanoscale* **2015,** *7*, 6311-6318.
42. Reif, J.; Knaut, M.; Killge, S.; Winkler, F.; Albert, M.; Bartha, J. W., In Vacuo Studies on Plasma-Enhanced Atomic Layer Deposition of Cobalt Thin Films. *J. Vac. Sci. Technol. A* **2020,** *38*, 012405 1-9.
43. Van Hemmen, J.; Heil, S.; Klootwijk, J.; Roozeboom, F.; Hodson, C.; Van de Sanden, M.; Kessels, W., Plasma and Thermal ALD of Al2O3 in a Commercial 200 mm ALD Reactor. *J. Electrochem. Soc.* **2007,** *154*, G165.
44. Fomengia, G. N.; Nolan, M.; Elliott, S. D., First principles mechanistic study of self-limiting oxidative adsorption of remote oxygen plasma during the atomic layer deposition of alumina. *Phys. Chem. Chem. Phys.* . **2018,** *20*, 22783-22795.